



Improvement of Baker's yeast-based fuel cell power output by electrodes and proton exchange membrane modification

Ariadne H.P. de Oliveira^a, José J. Alcaraz-Espinoza^b, Mateus M. da Costa^b,
Marcio Luis F. Nascimento^a, Timothy M. Swager^c, Helinando P. de Oliveira^{b,*}

^a Programa de Pós-Graduação em Engenharia Industrial, Escola Politécnica, Universidade Federal da Bahia, 40210-630 Salvador, BA, Brazil

^b Instituto de Pesquisa em Ciência dos Materiais, Universidade Federal do Vale do São Francisco, Juazeiro, Bahia 48902-300, Brazil

^c Department of Chemistry and Institute for Soldier Nanotechnologies, Massachusetts Institute of Technology, 77 Massachusetts Avenue, Cambridge, MA 02139, United States

ARTICLE INFO

Keywords:

Yeast fuel cell
Energy generation
Biofilm
Impedance
Membrane

ABSTRACT

The production of more efficient yeast-based fuel cells (YFCs) depends on a combination of effective proton exchange membranes, electron mediators and current collectors. The adhesion of organisms on electrode surface plays a key role in the electron transfer process optimizing the generated power density. In this work, it is reported the preparation of a new YFC prototype using membranes of polyvinyl alcohol/ phosphoric acid and anodes of carbon nanotubes/polyurethane. The high surface area for yeast adhesion and the strong interaction established between cells/carbon nanotubes favor the energy generation in fuel cell. To evaluate the influence of external mediators and the consumption of feed solution (glucose) on performance of YFC, the kinetics of current generation of resulting fuel cells was analyzed. Results reveal that increases in the impedance of electrodes on generated power can be minimized by periodical infusion of feed fuel, preserving 70% of maximum power, representing an important condition for prolonged activity of fuel cell.

1. Introduction

To decrease reliance on petroleum derived hydrocarbons, new strategies for the use of bio-based fuel cells emerge as needed to develop sustainable and environmental friendly energy sources [1–5]. Although there has been considerable work on bacteria based biocatalytic systems [6], there has been scarce attention devoted to the yeast in spite of the fact that these non-pathogenic organisms are easily handled and display high growth rates. Yeast is an inexpensive, readily cultivated organism with broad feed solution (fuel) scope that can deliver promising results in electricity generation.

Electron transfer processes in YFCs are formally involved in ATP synthesis, including the conversion of NAD^+ to NADH. The process of electrical current generation requires the diversion of these electron transfer processes to electrodes. These mechanisms occur by direct transference from bounded membrane – cytochromes/ electrically conductive pili, the action of exogenous redox mediators or the oxidation of reduced metabolites. There are scarce exoelectrogens to provide the electron transfer without redox mediators (electron shuttles) [7].

For electron shuttle-mediated processes, reduced electron shuttles

(ES_r) are produced by the internal processes in microorganisms and diffuse from cells to electrodes wherein charge transfer takes place, generating oxidized electron shuttles (ES_o) that can then be reduced again [8]. The optimal pairing of *Saccharomyces cerevisiae* cells and the electron mediator methylene blue (MB) [9,10] ($E^0 = 0.011$ V) is confirmed by the measured reduction potential of the succinate/fumarate [11] complex ($E^0 = 0.03$ V).

The general YFC design consists in a two-chamber assembly with microorganisms enclosed in an anaerobic compartment (anode) and a cathode in an aerated compartment. Charge dissipation is required between the compartments and they must be connected by ion (proton or cation) exchange membrane or a salt bridge [12–15]. The most common assembly, using proton exchange membranes, is schematically drawn in Fig. 1. Commercially available state-of-the-art membranes suitable for YFC are humidified perfluorosulfonic acid (Nafion) membranes, which exhibit a high proton conductivity and chemical stability. However, Nafion membranes have the disadvantages of relatively high cost, the need for humidification, susceptibility to biofouling, and high methanol crossover.

To circumvent the aforementioned membrane disadvantages, other polymeric materials have been modified to create membrane materials

* Corresponding author.

E-mail address: helinando.oliveira@univasf.edu.br (H.P. de Oliveira).

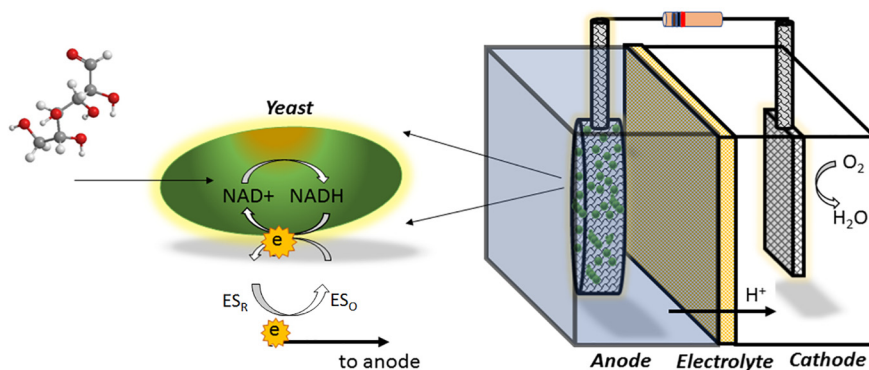


Fig. 1. Scheme of electron transfer from yeast cell to anode and the prototype of dual-chamber biologic fuel cell.

through chemical functionalization, blending, or through additives. Poly (vinyl alcohol) (PVA) is a promising candidate to host polymers and acids [16], as a result of its characteristic high chemical stability, intrinsic hydrophilicity, good film forming ability, excellent electrical resistance, low cost, good mechanical properties, and ability to be crosslinked by many different chemical functional groups and chemical processes [17].

The good electrochemical response of PVA-based membranes for YFC was recently explored in our group [18], characterizing blends of PVA and sulfonic acid groups (polystyrene sulfonic acid) crosslinked with glutaraldehyde as promising candidates for membrane, exhibiting a low swelling ratio in methanol, improved thermal stability, and high ionic conductivity. The synergistic combination of PSS-PVA imparts hydrophilic character on one side the membrane and compensates for proton exchangeable sites that are lost during the crosslinking process.

Moreover, the membrane proton conductivity can be improved by doping the non-crosslinked PVA fraction with acid solution [19]. Here, the association of the PSS-PVA and H_3PO_4 results in a blend with improved proton conductivity in dehydrated as well as hydrated states, with an estimated ionic transference number in order of 0.97 [20], thereby qualifying a promising PEM candidate with excellent thermal, chemical and electrochemical stability [21].

Another noticeable feature, it is that the hydrophilic character of the resulting polymeric membranes produces an antifouling effect, a highly desired characteristic of PEMs applied to microbial fuel cells. The high density of $-OH$ in PVA and the presence of water molecules in the structure of membrane favor the increase in the proton conductivity of PSS-PVA- H_3PO_4 membranes [22].

The improvement in the power density in MFCs can also be achieved by increasing the electrode surface area. Specifically, incorporating carbon nanotubes in electrodes improves the electrical conductivity and surface area. Matsumoto et al. [23] reported the formation of a 3D conductive network of CNT and *S. cerevisiae* and found strong interactions between the cells and the CNTs surface [23].

In this work, it is explored an optimized configuration of a two-chamber YFC using Baker's yeast (*S. cerevisiae*) in association with an electron shuttle (MB), electrodes formed from polyurethane/carbon nanotubes (PU/CNT) composites, and PEM membranes from a blended crosslinked PSS-PVA with added H_3PO_4 . The configuration combines the characteristic porous structure of PU/CNT and low cost PVA-based PEMs to provide a new alternative platform that associates high power density generation with low material costs.

2. Materials and methods

2.1. Materials

K_2HPO_4 (Potassium hydrogen phosphate) (Isobar Inc), EDTA (2,2',2'',2'''-(Ethane-1,2-diyl)dinitrilo)tetra acetic acid) (Neon Chemicals) and HCl (Neon Chemicals), Sabouraud 4% dextrose agar

(Merck), potassium hydroxide and acetone (Exodo Scientific), phosphoric acid (Dinamica Quimica), poly(vinyl alcohol), poly(4-styrenesulfonic acid) solution, glutaraldehyde, methylene blue, D-(+)-glucose, sodium dodecyl benzene sulphonate (SDBS) and multi-walled carbon nanotubes (Sigma-Aldrich) were used as received. Dissolved oxygen was measured using Multiparameter Analyzer Hanna HI9829 (Hanna Instruments), open cell voltage was measured by Keithley Multimeter 2002, generated power was measured using a Potentiostat Galvanostat Autolab Metrohm PGSTAT302N, the kinetics of yeast growth were measured by absorbance of feed solution at 273 nm in a spectrophotometer Hach DR5000, microstructure of electrodes and membrane was provided by Raman spectrum measurement performed in a LabRAM HR Evolution Raman Spectrometer Horiba Scientific. The morphology of electrodes was analyzed in a Scanning Electron Microscope (Vega 3XM Tescan at accelerating voltage of 20 kV).

2.2. Yeast solution preparation

The culturing of *S. cerevisiae* was performed as follows: the feed solution (Sabouraud 4% dextrose agar) - SDA was sterilized in an autoclave chamber for 15 min (115 °C) to avoid bacterial contamination in yeast media. The mother strain *Saccharomyces cerevisiae* cepa 1026 (Alltech, Brazil) was inoculated in a Petri dish containing feed solution using a sterile platinum loop. Resulting material was incubated at 30 °C for 24 h after that aliquots of material were dispersed in 0.1 M potassium phosphate dibasic buffer (pH 7) at 25 °C (anolyte solution) in the presence/ absence of external electron shuttle (methylene blue).

2.3. PEM preparation

An aqueous solution of PVA (0.2%) was kept in a thermal bath for 2 h at 90 °C for complete dispersion of polymer. After this step, 2 mL of poly (4-styrenesulfonic acid) (PSSA) is introduced into aqueous solution of PVA (10 mL) under intense stirring. The resulting solution was poured into a Petri dish and allowed to set for 48 h at 25 °C, which resulted in complete solvent evaporation. The PVA/PSSA film was carefully peeled off Petri dish surface. The membrane was crosslinked by immersion in glutaraldehyde solution (10%), containing 50 μ L of HCl (0.1 M) and 10 mL of acetone for 1 h at 25 °C. After this step, the resulting material is washed with milli-Q water [24]. As a final step for acidic groups incorporation, the crosslinked membrane is immersed in a H_3PO_4 aqueous solution (4 M) [25] for 24 h. The PVA/ H_3PO_4 membrane is washed with milli-Q water for the elimination of unbound phosphoric acid.

2.4. Anode electrodes preparation

The anodic collector electrode was prepared using a commercial microporous polyurethane sponge, which is gently washed with water

and alcohol several times before the CNT incorporation procedure. Carbon nanotubes were impregnated into the polyurethane microstructure according to the procedure reported by Xie et al. [26]: the dispersion of carbon nanotubes in solution is provided by sonication of a multiwalled carbon nanotubes (MWCNT): sodium dodecylbenzenesulphonate (SDBS) aqueous solution (0,1% of MWCNT in 1% SDBS w/w) for 30 min. The PU sponge is immersed into the CNT/SDBS solution under sonication for 5 min to incorporate carbon nanostructures. The resulting PU/CNT composite is dried at 90 °C and this process of CNT incorporation is repeated three times for each electrode. The resulting samples are washed in alcohol and water. The residual solvent evaporation is established under room conditions.

2.5. Dual chamber YFC prototype assembly

The YFC was prepared using two cylindrical chambers fabricated from Teflon (internal volume of 40 mL/ external and internal diameter of 9 cm and 5 cm, respectively). The electrodes immersed into the cell were a composite of PU/CNT as anode and a circular disc (50 mm of diameter) of carbon cloth (20% platinum on Vulcan carbon (Fuel Cell Store) as cathode). The separation membrane (PVA/H₃PO₄ membrane) is placed between with chambers and two acrylic plates are used to seal the device.

2.6. Anolyte solution preparation

The anolyte is composed by 40 mL of buffer solution pH 7 (K₂HPO₄ (0.1 M) and EDTA (0.1 mol/L)), glucose (0.5 g), *S. cerevisiae* (0.038 g) and MB(0.3 mM) [9].

3. Results

3.1. Electrodes characterization

The morphology of pristine electrodes of polyurethane (PU) and composites of PU/CNT were characterized by SEM image analysis. The structure of microporous cavities of polyurethane sponge is shown in Fig. 2a. The progressive incorporation of carbon nanotubes on these structures confirms the favorable adhesion of MWCNTs (see Fig. 2b) to provide high surface area electrode. Inspection of Fig. 2c further reveals the complete uniform coverage of PU with MWCNT. The abundance of MWCNTs on PU surface facilitates yeast adhesion and high conductivity of resulting material.

The PU/MWCNT electrode was also analyzed from Raman spectroscopy. The spectra of the base electrode (pristine PU) was compared with the modified PU/MWCNT composite. The results for the pristine PU in Fig. 3 reveal characteristic peaks of hard segments of pristine polyurethane electrodes, viz. C–N stretching vibration at 1277 cm⁻¹, CH₂ wagging/twisting mode at 1316 cm⁻¹, C–N stretching vibration and N–H bending vibration at 1535 cm⁻¹, and C=C stretching vibration from aromatic ring at 1612 cm⁻¹ [27]. The spectrum of PU/

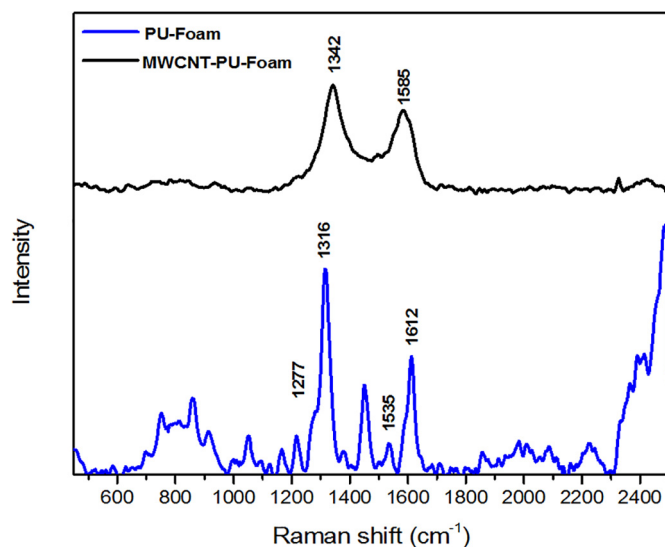


Fig. 3. Raman spectrum of polyurethane sponge and PU/CNT composite.

MWCNT composite is characterized by typical signature of sp² carbon materials with an in-plane vibration of the C–C bond (G band) at 1585 cm⁻¹ and disorder-induced D-band at 1342 cm⁻¹ [28], characterizing the presence of carbon nanotubes on PU surface. The absence of characteristic PU peaks in the PU/MWCNT spectrum indicates the high degree of coverage of the carbon nanotubes on the electrode surface. In addition to the adequate characterization of electrodes, the kinetics of yeast growth represents a critical process to be considered in the optimization of the YFC performance.

3.2. Yeast growth kinetics

The kinetics of yeast growth was monitored from a control experiment in which Baker's yeast was added to a glucose aqueous solution. In order to identify the kinetics of microorganisms' growth the concentration of dissolved oxygen was monitored in solution from corresponding level of optical density – measurement of absorbance of characteristic peak from yeast. The oxygen measurements reflect the total population including those cells that bind initially to the electrode while the optical measurements in solution represent freely suspended yeast. There a latency in the cell proliferation (adaptation and growth of individual fungi, which is followed by exponential growth wherein the cell doubling rate is strongly affected by its surroundings). The reduction of dissolved oxygen indicates can be used to monitor this process (results shown in Fig. S11) [29–31].

The comparison with control experiments, wherein no microorganisms are incorporated in the feed solution, reveal negligible variation in the dissolved oxygen concentration with time, confirming that the oxygen consumption in the yeast containing devices is the result of

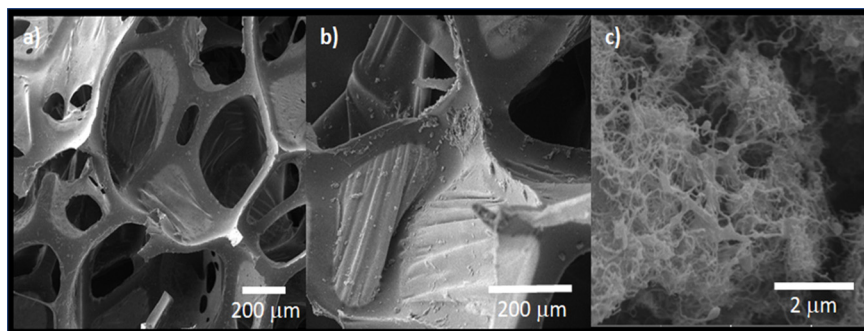


Fig. 2. SEM images of pristine polyurethane sponge - PU (a), covered PU with carbon nanotubes (b and c).

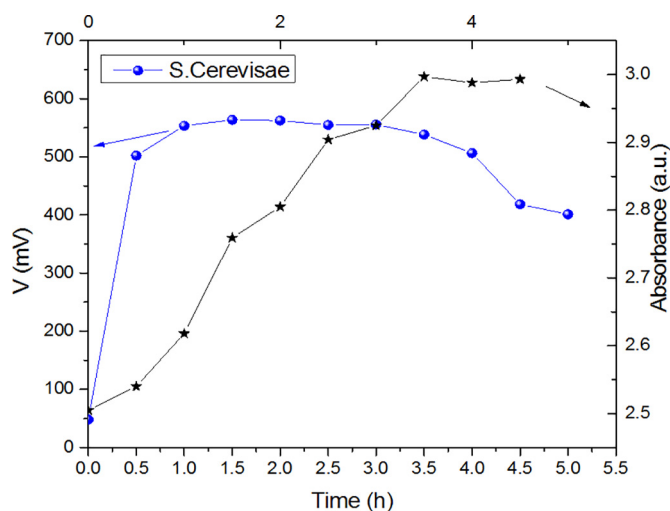


Fig. 4. Generated OCV (in blue) and absorbance (at 273 nm) – in black for feed solution (absence of external mediator) as function of time of reaction. (For interpretation of the references to colour in this figure legend, the reader is referred to the web version of this article.)

cell respiration processes. Moreover, if considered the corresponding experiment performed in the presence of electrodes (curve in green) it is possible to observe the same behavior (the dissolved oxygen concentration tends to zero for corresponding interval of time), confirming that presence of electrodes affects minimally the kinetics of yeast growth.

The yeast growth rate can be measured from monitoring the optical density/absorption of solution: the variation in the absorbance peak at 273 nm was explored for identification of yeast concentration in feed solution. As can be seen from results in Fig. 4, the minimal lag time ($t < 0.5$ h) is followed by strong variation in the absorbance level. This process reaches an end at time $t = 3.5$ h, which corresponds to a point wherein the dissolved oxygen is at a minimum. The arresting of the yeast doubling process indicates that oxygen consumption acts as growth-limiting factor, wherein the growth-rate and the death-rate of yeast cells are balanced. This behavior is observed in the response of assembled YFC (overall systems with membrane and electrodes) - the measured open-cell voltage between anode and cathode (left-axis in Fig. 4) reaches a constant value at this time (in the absence of methylene blue) at ≈ 0.55 V.

3.3. Biofilm formation on electrodes

The saturation in the yeast growth rate is followed by the adhesion of yeast cells on PU/CNT electrodes. The latter process is critical to efficient mediated electron transfer process from internal yeast to the anode. After 24 h, the electrode surfaces are progressively covered by yeast binded to the nanoporous roughend surface. SEM Images in Fig. 5a, b and c show the adhesion of yeast cells to carbon nanotubes in PU/MWCNT electrodes. If considered the prolonged interaction of yeast cells and electrodes, the continuous incorporation of microorganisms on the anode results in the formation of a complete biofilm (Fig. 5d–f), indicating a modification in the growth rate of microorganisms from liquid to the electrode's surface. It is expected that the electrical resistance of electrodes will also be affected by the extracellular substances covering on MWCNT.

The identification of living yeast cells on electrodes under prolonged operation was evaluated as follows: after ten days of continuous use of YFC prototype, the electrodes were immersed in milli-Q water under mechanical agitation for removal of microorganisms from electrodes' surface. The resulting solution was plated in SDA and incubated at 37 °C. After 48 h of inoculation, it is possible to identify the regular

growth of *Saccharomyces cerevisiae* disposed on electrodes (see Fig. SI 2b) while the corresponding process for pristine electrodes (negative control) returned the complete absence of microorganisms (see Fig. SI 2a). It is a proof that viable yeast cells are present on surface of electrodes under continuous operation, characterizing low toxicity degree of mediator and materials explored in the YFC prototype.

Moreover, the presence of external electron shuttle (in addition to the EDTA – buffer solution) and feed solution rate represent additional critical parameters for the optimization of the generated power. To this end, it was determined a combination of parameters for the operation of high-performance devices. The influence of external mediator on power generation value was analyzed from experiments in which the response of similar YFCs was compared in the presence/absence of the MB.

3.4. Influence of electron shuttles on YFC performance

Results in Fig. 6a confirm that addition of MB as electron mediator improves both the voltage and current (under open circuit and short circuit condition) thereby indicating that redox molecules play a critical role in cell-to-electrode electron transfer. As shown in the Fig. 6b, the incorporation of MB contributes to a two-fold increase in the maximum power. These results confirm that although the EDTA can participate as a primary electron shuttle agent for electron transfer in YFC prototype, others will require additional mediated electron transport process to deliver electrons to the anode.

It is worth mentioning that bakers' yeast-based fuel cells depend on incorporation of exogenous compounds for hijacking electrons accumulated in NADH due to the non-conductive surface of yeasts lipid membrane that hinders the direct transference of electrons to anode [3,9,32,33]. It is reported the use of different exogenous compounds with different level of toxicity – with direct impact on prolonged generation of energy [32]. For anolyte, we explored the use of two electron shuttles (EDTA and methylene blue) characterized by low toxicity degree [32]. Moreover, the control in the pH value favors the transport of methylene blue through cytoplasmic membrane, allowing the synergistic interaction of EDTA and methylene blue as exogenous compounds favoring electrons transport.

3.5. Prolonged electron transfer in YFC

The influence of the fuel (glucose) feed-rate on electricity generation was analyzed in experiments wherein the response of corresponding cells was monitored under periodic feed fuel injection and restricted feed injection. In the first condition, 90% of anolyte solution was substituted (electron mediator + glucose) at fixed interval of 24 h. In the second condition, the cells are given a single injection of feed and the device is monitored over 24 h intervals.

The results shown in Fig. 7 reveal that decrease in the maximum voltage and current are observed with the progressive consumption of feed fuel and additional biofilm growth on electrodes, characterizing collaborative variables responsible for decreasing performance of YFC (Fig. 7a). The progressive biofilm formation affects the internal resistance of electrodes, which reduces current and energy conversion efficiency (Fig. 7a). As expected, the maximum power is observed in the day #1, in which the feed concentration is maximum and planktonic form of cells prevails over biofilm formation, thereby preserving the high conductivity of electrodes (Fig. 7b). The decreasing power for successive days after feed process can be attributed to two different mechanisms: -the increase in the impedance of electrodes (progressive biofilm deposition) and the decrease of available feed fuel.

The measured impedance of fuel cell as a function of time is shown in Fig. 7c. A decrease in the real part of impedance of device in the first 24 h of activity is attributed to the intense reproductive behavior of yeast cells in planktonic form after inoculation. The minimal adhesion of cells on electrodes favors the increase in the particles density (yeasts) in the bulk solution, provoking the decrease in the cell impedance. After

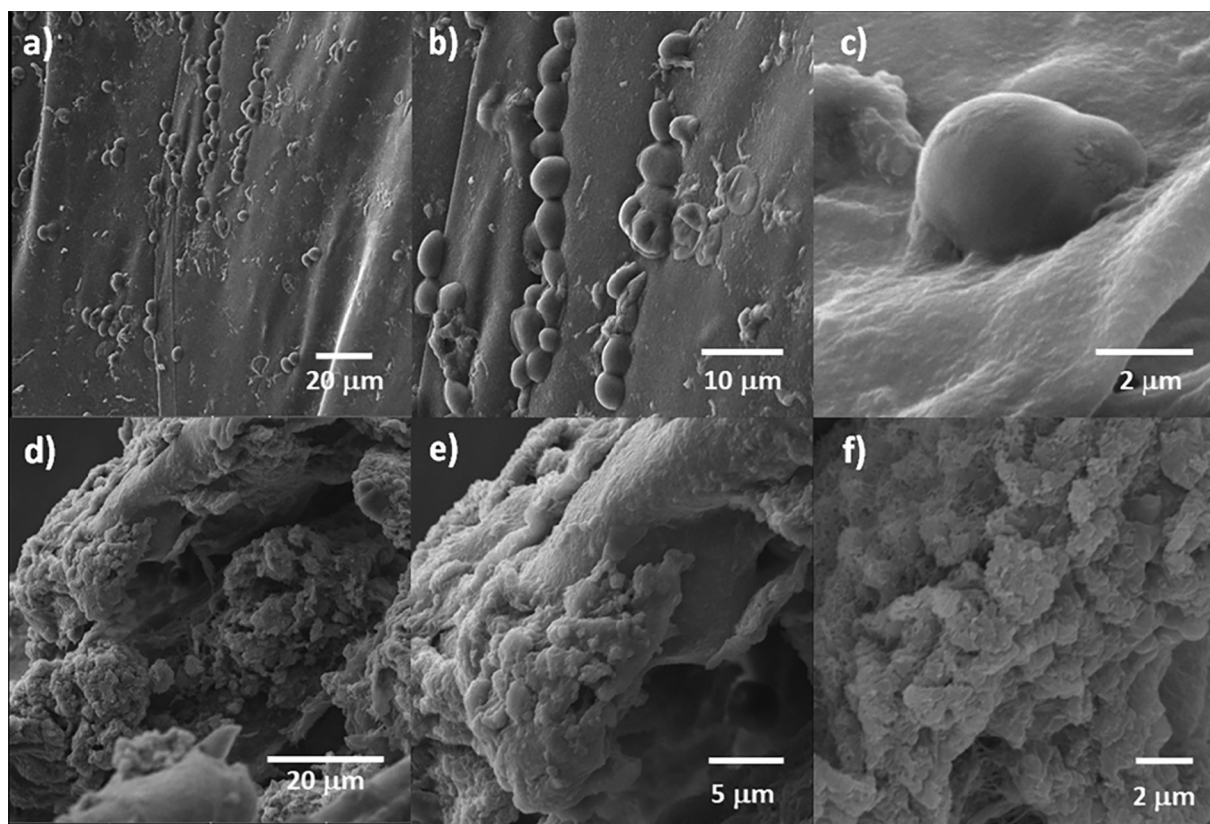


Fig. 5. SEM images of anode after 24 h of use in YFC (a), (b), (c) and after 10 days of reaction in YFC (d), (e) and (f) at different magnification.

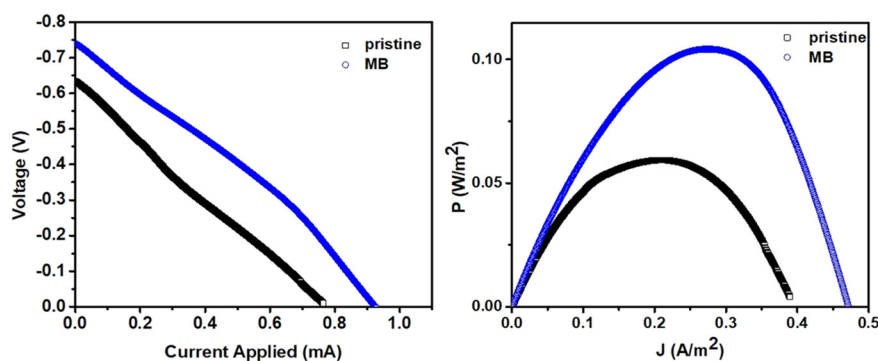


Fig. 6. (a) Voltage vs. current curve of YFC in the presence/absence of external mediators (b) comparison of generated power in the absence/presence of external mediator – methylene blue. (For interpretation of the references to colour in this figure legend, the reader is referred to the web version of this article.)

the first day, the saturation in the yeast growth rate and progressive deposition of cells on electrodes affects the impedance of fuel cell and results in decreasing Z' value relative to that measured in the first day of operation. The higher impedance contributes to the decrease in generated power, and after 48 h of fuel insertion, the generated power is reduced by a factor of 2 (Fig. 7d).

In order to estimate the relevance of these two limiting factors on available power on YFCs, it was compared the response of devices that had a single initial fuel insertion, with devices wherein 90% of anolyte was replaced every 24 h with a fresh glucose/MB solution. The results in Fig. 7d confirm that under both conditions the maximum power is obtained in the first day of cell operation. The saturation in the yeast cell production reduces the power to values in order of 70% of the maximum, that remains constant with continuous substitution of glucose/MB. The increasing impedance level of fuel cell can be circumvented by periodical glucose incorporation. The compromised electrical response of electrodes is balanced by efficient electron

transfer process from entrapped yeast cells to the anode mediated by MB. This allows the YFCs to operate at 70% of maximum power of YFC ($100 \text{ mW}/\text{m}^2$) for long periods with periodic substitution of fuel and electron transfer shuttles. These chemical properties open new possibilities for use of this membrane and overall prototypes in applications such as in the treatment of synthetic wastewater.

4. Conclusion

The carbon nanotube impregnated polyurethane sponges offer an efficient environment for yeast adhesion under anaerobic conditions in anolyte solutions. The dual chamber yeast-based fuel cell incorporates a PVA + H_3PO_4 PEM membrane, and provides a sustained power output of approximately $100 \text{ mW}/\text{m}^2$. In spite of progressive biofilm accumulation and increasing impedance of electrodes, the strategy of daily substitution of anolyte (electron mediator and feed) preserves the activity of the biocatalytic activity, that produces electricity at 70% of the

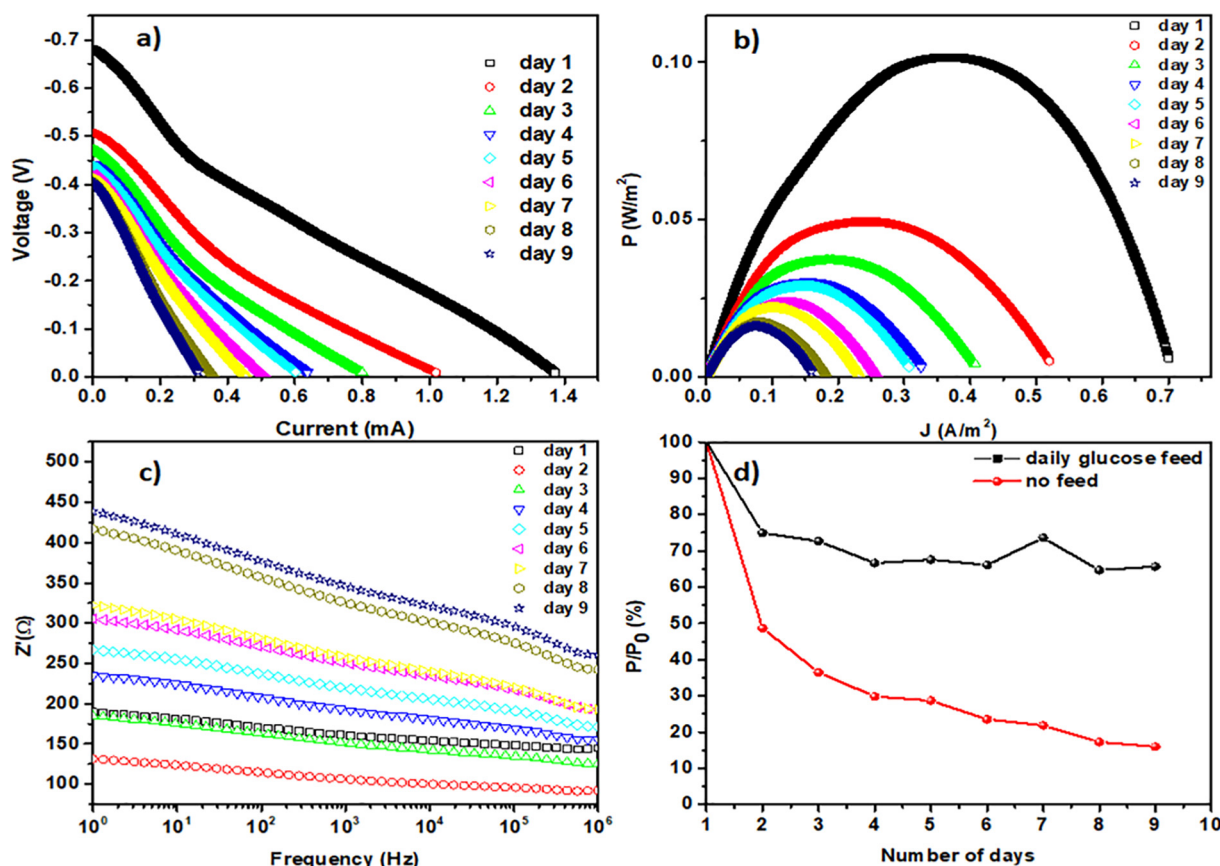


Fig. 7. (a) Voltage/current of YFC as function of days after feed fuel insertion, (b) corresponding power of YFC, (c) real part of impedance of YFC as function of time of feed fuel insertion and (d) dependence of relative power of YFC in terms of the first day generation with dairy feed fuel and no feed fuel.

maximum power observed on the first day. The designed YFC assembly provides a new perspective for the scalable application of low-cost devices in energy generation processes.

Acknowledgment

This work was partially supported by the Brazilian agencies FINEP, CAPES, FAPESP, FACEPE, CNPq and MISTI MIT-Brazil Seed Fund.

Declaration of competing interest

The authors have no affiliation with any organization with a direct or indirect financial interest in the subject matter discussed in the manuscript.

Appendix A. Supplementary data

Supplementary data to this article can be found online at <https://doi.org/10.1016/j.msec.2019.110082>.

References

- [1] S. Holmberg, A. Perebikovskiy, L. Kulinsky, M. Madou, 3-D micro and nano technologies for improvements in electrochemical power devices, *Micromachines - Basel* 5 (2) (2014) 171–203.
- [2] C.P.B. Siu, M. Chiao, A Microfabricated PDMS Microbial Fuel Cell, *J. Microelectromech. Syst.* 17 (6) (2008) 1329–1341.
- [3] A. Gunawardena, S. Fernando, F. To, Performance of a yeast-mediated biological fuel cell, *Int. J. Mol. Sci.* 9 (10) (2008) 1893–1907.
- [4] E.T. Sayed, N.A.M. Barakat, M.A. Abdelkareem, H. Fouad, N. Nakagawa, Yeast extract as an effective and safe mediator for the Baker's-yeast-based microbial fuel cell, *Ind. Eng. Chem. Res.* 54 (12) (2015) 3116–3122.
- [5] M. Chiao, K.B. Lam, L.W. Lin, Micromachined microbial and photosynthetic fuel cells, *J. Micromech. Microeng.* 16 (12) (2006) 2547–2553.
- [6] P. Banerjee, S.R. Barman, S. Swarnakar, A. Mukhopadhyay, P. Das, Treatment of textile effluent using bacteria-immobilized graphene oxide nanocomposites: evaluation of effluent detoxification using *Bellamyia bengalensis*, *Clean Technol. Environ.* 20 (10) (2018) 2287–2298.
- [7] S.A. Patil, C. Hägerhäll, L. Gorton, Electron transfer mechanisms between microorganisms and electrodes in bioelectrochemical systems, *Bioanal. Rev.* 4 (2–4) (2012) 159–192.
- [8] A. Szollosi, Q.D. Nguyen, A.G. Kovacs, A.-L. Fogarasi, S. Kun, B. Hegyesne-Vecseri, Production of low or non-alcoholic beer in microbial fuel cell, *Food Bioprod. Process.* 98 (2016) 196–200.
- [9] M. Rahimnejad, G. Najafpour, A. Ghoreysy, M. Shakeri, H. Zare, Methylene blue as electron promoters in microbial fuel cell, *Int. J. Hydrogen Energy.* 36 (20) (2011) 13335–13341.
- [10] D. Malik, S.S. JayitaThakur, R.K. Singh, A. Kapur, A. Kaur, A.K. Nijhawan, Nanocomposite electrode microbial fuel cell: a promising technology for enhanced power generation from Yamuna water, *Int. J. Sci. Res.* 3 (7) (2014) 641–646.
- [11] O. Schaeztle, F. Barrière, K. Baronian, Bacteria and yeasts as catalysts in microbial fuel cells: electron transfer from micro-organisms to electrodes for green electricity, *Energy Environ. Sci.* 1 (6) (2008) 607–620.
- [12] D. Permana, D. Rosdianti, S. Ishmayana, S.D. Rachman, H.E. Putra, D. Rahayuningwulan, H.R. Hariyadi, Preliminary investigation of electricity production using dual chamber microbial fuel cell (DCMFC) with *saccharomyces cerevisiae* as biocatalyst and methylene blue as an electron mediator, in: H. Hayashi, R. Read, K. Awang (Eds.), 3rd International Seminar on Chemistry 2014, Elsevier Science Bv, Amsterdam, 2015, pp. 36–43.
- [13] Y.J. Zou, J. Pisciotto, I.V. Baskakov, Nanostructured polypyrrole-coated anode for sun-powered microbial fuel cells, *Bioelectrochem* 79 (1) (2010) 50–56.
- [14] D.L. Zugic, I.M. Perovic, V.M. Nikolic, S.L. Maslovara, M.P.M. Kaninski, Enhanced performance of the solid alkaline fuel cell using PVA-KOH membrane, *Int. J. Electrochem. Sci.* 8 (1) (2013) 949–957.
- [15] A.Y. Cetinkaya, B. Ozkaya, E. Taskan, D. Karadag, M. Cakmakci, The production of electricity from dual-chambered microbial fuel cell fueled by old age leachate, *Energy. Source. Part A* 38 (11) (2016) 1544–1552.
- [16] G. Chen, B. Wei, Y. Luo, B.E. Logan, M.A. Hickner, Polymer separators for high-power, high-efficiency microbial fuel cells, *ACS Appl. Mater. Interf.* 4 (12) (2012) 6454–6457.
- [17] Y.-S. Ye, J. Rick, B.-J. Hwang, Water soluble polymers as proton exchange membranes for fuel cells, *Polymers* 4 (2) (2012) 913–963.
- [18] A.H.P. de Oliveira, M.L.F. Nascimento, H.P. de Oliveira, Preparation of KOH-doped PVA/PSSA solid polymer electrolyte for DMFC: the influence of TiO₂ and PVP on performance of membranes, *Fuel Cells* 16 (2) (2016) 151–156.

- [19] F. Ahmad, E. Sheha, Preparation and physical properties of (PVA) 0.7 (NaBr) 0.3 (H₃PO₄) x M solid acid membrane for phosphoric acid–fuel cells, *J. Adv. Res.* 4 (2) (2013) 155–161.
- [20] M. Rikukawa, K. Sanui, Proton-conducting polymer electrolyte membranes based on hydrocarbon polymers, *Prog. Polym. Sci.* 25 (10) (2000) 1463–1502.
- [21] S. Dharmadhikari, P. Ghosh, M. Ramachandran, Synthesis of proton exchange membranes for dual-chambered microbial fuel cells, *J. Serb. Chem. Soc.* 83 (5) (2018) 611–623.
- [22] S. Khilari, S. Pandit, M.M. Ghangrekar, D. Pradhan, D. Das, Graphene oxide-impregnated PVA–STA composite polymer electrolyte membrane separator for power generation in a single-chambered microbial fuel cell, *Ind. Eng. Chem. Res.* 52 (33) (2013) 11597–11606.
- [23] S. Matsumoto, K. Yamanaka, H. Ogikubo, H. Akasaka, N. Ohtake, Carbon nanotube dispersed conductive network for microbial fuel cells, *Appl. Phys. Lett.* 105 (8) (2014) 083904.
- [24] J. Fu, J. Qiao, X. Wang, J. Ma, T. Okada, Alkali doped poly (vinyl alcohol) for potential fuel cell applications, *Synth. Met.* 160 (1) (2010) 193–199.
- [25] G. Merle, M. Wessling, K. Nijmeijer, Anion exchange membranes for alkaline fuel cells: a review, *J. Memb. Sci.* 377 (1–2) (2011) 1–35.
- [26] X. Xie, M. Ye, L. Hu, N. Liu, J.R. McDonough, W. Chen, H.N. Alshareef, C.S. Criddle, Y. Cui, Carbon nanotube-coated macroporous sponge for microbial fuel cell electrodes, *Energy Environ. Sci.* 5 (1) (2012) 5265–5270.
- [27] S. França de Sá, J.L. Ferreira, A.S. Matos, R. Macedo, A.M. Ramos, A new insight into polyurethane foam deterioration—the use of Raman microscopy for the evaluation of long-term storage conditions, *J. Raman Spect.* 47 (12) (2016) 1494–1504.
- [28] M. Dresselhaus, G. Dresselhaus, A. Jorio, A. Souza Filho, R. Saito, Raman spectroscopy on isolated single wall carbon nanotubes, *Carbon* 40 (12) (2002) 2043–2061.
- [29] F.F. Aceituno, M. Orellana, J. Torres, S. Mendoza, A.W. Slater, F. Melo, E. Agosin, Oxygen response of the wine yeast *Saccharomyces cerevisiae* EC1118 grown under carbon-sufficient, nitrogen-limited enological conditions, *Appl. Environ. Microb.* 78 (23) (2012) 8340–8352.
- [30] J. Strohm, R. Dale, Dissolved oxygen measurement in yeast propagation, *Ind. Eng. Chem.* 53 (9) (1961) 760–764.
- [31] A. Baez, J. Shiloach, Effect of elevated oxygen concentration on bacteria, yeasts, and cells propagated for production of biological compounds, *Microb. Cell Factories* 13 (1) (2014) 181.
- [32] A. Adebule, B. Aderiye, A. Adebayo, Improving bioelectricity generation of microbial fuel cell (MFC) with mediators using kitchen waste as substrate, *Ann. Appl. Microbiol. Biotechnol.* J 2 (1) (2018) 1–5.
- [33] R. Rossi, A. Fedriguccia, L. Settia, Characterization of electron mediated microbial fuel cell by *Saccharomyces cerevisiae*, *Chem. Eng. Trans.* 43 (2015) 337–342.